CHEMICAL ENGINEERING TRANSACTIONS
VOL. 117, 2025
A publication of AIDIC
The Italian Association of Chemical Engineering
Online at www.cetjournal.it
Guest Editors: Fabrizio Bezzo, Flavio Manenti, Gabriele Pannocchia, Almerinda di Benedetto

ISBN 979-12-81206-17-5; **ISSN** 2283-9216
DOI: 10.3303/CET25117137

Multi-Metal Oxides used as Catalyst and Oxygen Carrier for Reforming and Partial Oxidation of Bio-Methane

Francesco Miccio[a,*], Lucrezia Polchri[a], Giuseppina Iervolino[b], Frédéric Monteverde[a]

[a]Institute of Science, Technology and Sustainability for Ceramics (ISSMC), National Research Council of Italy (CNR), Via Granarolo, 64, 48018 Faenza, RA, Italy.
[b]Department of Industrial Engineering, University of Salerno, via Giovanni Paolo II, 132, SA, Fisciano, 84084, Italy.
francesco.miccio@cnr.it

Partial oxidation and reforming of methane are well-known methods to obtain mixtures of CO, CO_2 and H_2 that can be separated or used in other processes, e.g. the synthesis of methanol. The aim of this study is to go beyond commercially available catalysts containing critical and expensive raw ingredients and find new, cheaper and more durable candidates for reforming and partial oxidation.
A multi-metal oxide (MMO), mostly known like “high-entropy” oxide, was developed, free of noble metals through conventional a solid-state reaction synthesis, and compared to some mixtures made of widely used oxides here reported: CeO_2/Al_2O_3, $CeO_2/Al_2O_3/CuO$ and $CeO_2/Al_2O_3/CuO/Ca(OH)_2$. The performance of the MMO was studied and compared to the oxide mixtures above reported. The materials were obtained as discrete granules of irregular shape in the range of 1-2 mm by pelletizing them and further hot consolidation. TPR analysis and tests in a laboratory scale quartz reactor with feeding lines of different gas mixtures were carried out. Promising results in terms of reducibility, CH_4 conversion (up to 95%) and CO selectivity (up to 60%) were achieved for CeO_2/Al_2O_3 and MMO, the latter showing good behavior over repeated cycles.

1. Introduction

Using renewable methane (CH_4) from biogas purification is a route to produce green H_2 by partial oxidation, thermal decomposition and steam or dry reforming (Lunsford, 2000). In particular, reaction R1 offers the possibility to exploit CO_2 from capture, and avoid its storage, although the endothermicity needs high temperature and external heat supply.

$$CH_4 + CO_2 \leftrightarrow 2CO + 2H_2 \qquad \Delta H°_{298\,K} = +247\ \frac{kJ}{mol} \quad (R1)$$

Partial oxidation and dry reforming of CH_4 assisted by an oxygen carrier are appealing for production of H_2 and CO mixtures, that can be used subsequently, e.g. for methanol synthesis. This process exploits the CH_4 partial oxidation (R2), an exothermic reaction that is energetically favored compared to the endothermic steam reforming and provides H_2/CO ratio of 2 (R3). The solid-state oxygen carrier is an alternative to the expensive pure oxygen, when the carrier also acts as catalyst toward CH_4 reforming, as in the case of Ni oxide (Zhang et al., 2021). Therefore, a strategy to perform the process under less severe conditions is based on the use of materials, typically metal oxides or mixed oxides, capable of acting both as an oxygen source and as catalysts. Main critical aspects of such a process are temperature control, selectivity towards partial oxidation and carbon deposition that may occur either via thermal decomposition or Boudouard reaction.

$$CH_4 + \rho_j{}_\varsigma O_2 \leftrightarrow CO + 2H_2 \qquad \Delta H°_{298\,K} = -35.9\ \frac{kJ}{mol} \quad (R2)$$

$$CH_4 + 2O_2 \leftrightarrow CO_2 + 2H_2O \qquad \Delta H°_{298\,K} = -802.6\ \frac{kJ}{mol} \quad (R3)$$

Paper Received: 3 December 2024; Revised: 8 April 2025; Accepted: 30 May 2025
Please cite this article as: Miccio F., Polchri L., Iervolino G., Monteverde F., 2025, Multi-metal Oxides Used as Catalyst and Oxygen Carrier for Reforming and Partial Oxidation of Bio-methane, Chemical Engineering Transactions, 117, 817-822 DOI:10.3303/CET25117137

The development of new catalysts for the process is inspired by the scope to limit, or even avoid, the deposition of C on the surface catalysts and the substitution of noble or toxic elements, in compliance with the principles of green chemistry (Guo et al., 2021). The process intensification and control are also relevant issues in reforming, requiring the use of structured catalysts with high thermal conductivity (Palma et al., 2016). In this regard, chemical looping (CL) is considered a viable option for H_2 production in an intensified process scheme based on granular oxygen carriers (OCs). Since the process is heterogeneous, the reactants (CH_4 and OC) can be kept in contact at high temperature in a suitable reactor with moderate heat exchange, preferably in fluidized beds (Lyngfelt, 2013). The base concept is that the reaction can be divided into two separate steps by exploiting the redox properties of the OCs. First, CH_4 is partially oxidized, avoiding full oxidation, by reduction of OC (R4), then the reduced carrier is regenerated (oxidized) by contact with air, O_2, CO_2, or H_2O (R5). During the regeneration stage, carbon deposited can be removed by oxidation, thus limiting the accumulation over repeated cycles. It is worth nothing that there is no syngas dilution in nitrogen, when air regeneration is performed.

$$OC^{OX} + CH_4 \leftrightarrow OC^{RED} + CO + 2H_2 \quad (R4)$$

$$OC^{RED} + \rho_j{}_\varsigma O_2 \leftrightarrow OC^{OX} \quad (R5)$$

This article shows the results of an experimental research on purposely developed ceramic catalysts and oxygen carriers for the partial oxidation and reforming of CH_4. In particular, the development, characterization and functional tests of oxide mixtures inspired by Green Chemistry and characterized by a complex molecular structure are presented and discussed.

2. Materials and methods

The experimental research was carried out on a laboratory scale with purposely prepared catalysts, based on previous experiences in catalysis and chemical looping combustion.

2.1 Materials preparation

Four different materials acting as catalyst and oxygen carrier were produced, as reported in Table 1, in a granular form. Samples coded Ce-Al, Ce-Cu-Al and Ce-Cu-Ca-Al were mixed from commercial powders according to the ratio reported in Table 1. In the following the raw powders used: CeO_2 (PIKEM UK, purity 99.9%), Al_2O_3 (Martinswerk KMS96), CuO (Copper (II) oxide Merck purity min 99.0%), $Ca(OH)_2$ (Calcium Hydroxide for analysis EMSURE). After dry mixing, samples were pelletized, cold pressed linearly at 100 bar, grossly crushed and sieved to obtain irregular granules in the range of 1-2 mm. The granules obtained were heat treated in air at 1173 K for 30 minutes and finally air quenched. Conversely, the synthesis of MMO was different (Monteverde, 2024). A mixture of oxides indicated in Table 1 was intimately wet mixed in a planetary mill using ethanol, dried and thus pelletized according to the procedure above reported: the selected range was 2-3 mm. The granules of MMO were heat treated at 1473 K for 60 min and then air quenched: the fraction of granules between 1 and 2 mm was selected for further testing.

Table 1: Catalysts-oxygen carriers used in experiments: percentages (wt. %) refer to the oxides of the starting mixtures.

Name	CeO_2	CuO	$Ca(OH)_2$	Al_2O_3	Co_3O_4	MnO_2	ZnO	MgO
Ce-Al	70	-	-	30	-	-	-	-
Ce-Cu-Al	48	22	-	30	-	-	-	-
Ce-Cu-Ca-Al	40	18	12	30	-	-	-	-
MMO	-	21	-	-	21	23	25	10

2.2 Experimental facilities and procedure

Temperature Programmed Reduction (TPR) tests were performed by using a 500 $Ncm^3\ min^{-1}$ flow of a H_2/Ar (H_2 content 10% vol.), while temperature was increased up to 600°C with a rate of 5°C min^{-1}. Composition of the gas mixture flowing out the reactor was continuously monitored using a mass spectrometer (Hiden HPR20).

A fixed bed reactor (quartz tube 20 mm ID), enclosed within a tubular electric furnace, was used for transient tests of CH_4 conversion (Figure 1). The reactor was equipped at the bottom side of a ceramic porous setter, acting as support for the catalyst and as gas distributor. A K-type thermocouple attached to the outer wall of

the reactor monitored the reactor temperature near the bed. Mass flows of N_2/CH_4 (92/8% vol.), N_2 and dry air were supplied by Brooks mass flowmeters (MF1, MF2 and MF3). A volume of 7 mL of catalyst was used during all tests and the volume fractions of O_2, CO_2, CO, CH_4 and H_2 were determined by a continuous gas analyzer GEIT-3500, by sampling at the upper opening of the reactor, after filtration (see Figure 1). The tests were performed by switching gas mixtures between partial oxidation (N_2/CH_4) and carrier regeneration (air) for at least three times at the same temperature with intermediate N_2 purge. The conditions that were used in the various tests are reported in Table 2.

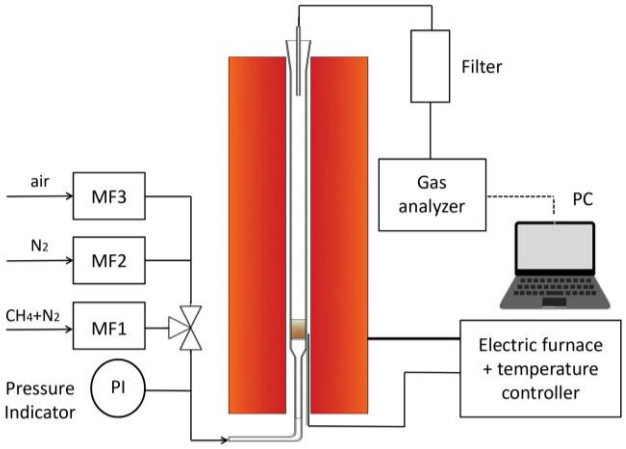

Figure 1: Experimental setup for partial oxidation and reforming of CH_4

The performance of the four materials was compared on the basis of main results: CH_4 conversion Eq(1), CO and H_2 yield Eq(2), whilst the carbon deposition was computed as 1 – $mmol_{Cout}$/ $mmol_{Cin}$.

$$CH_{\tau}conversion = \frac{mmolCH_{4_{IN}} - mmolCH_{4_{OUT}}}{mmolCH} \quad (1)$$

$$\eta CO, CH_2 = \frac{mmolCO_{OUT}, H_{2_{OUT}}}{mmolCH_{4_{IN}} - mmolCH_{4_{OUT}}} \quad (2)$$

3. Results

Figure 2 shows that, for the Ce-Al sample, the TPR analysis has a main peak of H_2 consumption between about 350 and 400 °C, indicating the reduction of CeOF ($Ce^{4}\phi \rightarrow Ce^{3}\phi$). The absence of well-defined multiple peaks suggests a surface reduction of CeOF. Furthermore, the profile in Fig. 2 exhibits a relatively gradual transition (250-300 °C) and a fairly broad peak, suggesting a moderate interaction between CeOF and $AlFO_F$, without a strong modification of the redox properties of Ce. The height of the peak (about 0.14% of H_2 consumed) indicates a moderate availability of reducible oxygen, consistent with non-promotable CeOF. Compared to a promotable system (e.g., with Cu or other metals), the amount of H_2 consumed is lower. After the main peak (> 450 °C), the H_2 consumption vanishes to negligible value. This indicates that the reduction is complete and that the material does not present other relevant reducible oxides. In the sample (Ce-Al) the presence of $AlFO_F$ does not seem to have a measurable influence in improving the oxygen availability of CeOF. However, it could contribute to the dispersion of CeOF and to the thermal stability of the material. CeOF shows its typical reduction at 350-400 °C, consistent with the known behaviour of Ce in the absence of promotion. The TPR plot of Ce-Cu-Al shows some distinctive features compared to the Ce-Al and allows to draw interesting observations on the effect of the presence of Cu on the redox behaviour of this material. The H_2 consumption peak is centred around 350 °C, 50 °C less than the reduction of CeOF in the Ce-Al sample (400 °C), proving that the presence of CuO plays a key role. Furthermore, the position of the peak is consistent with the reduction of CuO to Cu^0, favored by the interaction between Cu and CeOF. The peak is narrower and more defined than in the Ce-Al sample, suggesting a faster and more complete reduction of the material. This indicates that the reduction is dominated by the CuO phase, more easily reducible than CeOF. The peak exhibits a maximum H_2 consumption close to 2.5%, significantly higher than for Ce-Al. The presence

of Cu lowers the reduction temperature and enhances the redox activity of CeO_2, probably through the hydrogen spillover effect. During reduction, Cu promotes the mobility of hydrogen from the CeO_2 surface towards the CuO, lowering the overall reduction temperatures. After the main peak, H_2 consumption drops dramatically, suggesting completed reduction of the species. No significant signals are observed at higher temperatures, indicating that CeO_2 is poorly involved in the reduction of this configuration. Compared to Ce-Al, the Ce-Cu-Al sample shows higher redox activity (higher H_2 consumption) and better efficiency at low temperatures, confirming the role of Cu as a promoter of catalytic properties. In the case of the Ce-Cu-Ca-Al sample, multiple reduction peaks can be observed. In particular, two main reduction regions can be noted: A first peak (200-300 °C), very likely associated to the reduction of CuO to Cu^0, as already observed for the Ce-Cu-Al sample. The reduction temperature is consistent with the presence of CuO dispersed or interacting with CeO_2; second peak (300-450 °C) that can be attributed to the reduction of the CeO_2 phase, although it is influenced by the presence of Ca. The first peak is less defined than the Ce-Cu-Al sample, suggesting a less uniform reduction or a non-homogeneous distribution of CuO in the sample. This could be an effect of the introduction of calcium, which alters the structure of the catalyst. The total H_2 consumption is lower than the Ce-Cu-Al sample, Ca likely acting as a stabilizer and limiting the reducibility of CeO_2 and CuO. Furthermore, it could influence the dispersion of CuO or the formation of new complex Cu-Ca-O phases, which require higher temperatures for reduction.

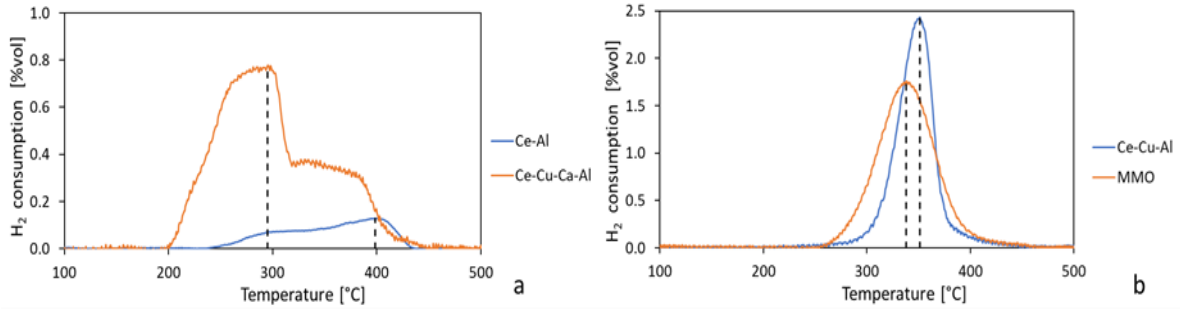

Figure 2: TPR analysis for the Ce-Al and Ce-Cu-Al, FS 1.0%vol. (a); Ce-Cu-Ca-Al and MMO, FS 1.0%vol. (b)

The TPR graph of MMO graph shows a main peak in H_2 consumption centred around 300-350 °C, due primarily to the reduction of CuO to Cu^0. Copper is known to be one of the most easily reducible metal oxides, with reduction typically occurring in such temperature range. Considering the composition of the sample MMO reported in Table 1, it is possible to distinguish the contribution of different components. In particular, the contribution of Co_3O_4 and MnO_2. As for Co_3O_4, it is reduced in two stages: $Co_3O_4 \rightarrow CoO$ (around 200-300 °C) and $CoO \rightarrow Co^0$ (around 350-450 °C). However, the presence of copper in this sample can lower the reduction temperature of Co_3O_4 thanks to the spillover effect of hydrogen, making it difficult to distinguish the two processes. MnO_2, on the other hand, begins to be reduced to Mn_2O_3 and subsequently to Mn_3O_4 between 300 and 400 °C, overlapping with the reduction process of CuO. For this reason, the main peak observed in the figure could be an overlap of the reductions of CuO, Co_3O_4 and MnO_2. As for ZnO and MgO, these oxides are hardly reducible and typically do not show obvious signs in TPR. MgO, being a basic oxide, does not participate in reduction reactions. The presence of multiple oxides (CuO, Co_3O_4, MnO_2) may result in a synergistic interaction. However, the closeness of the reduction temperatures for CuO, Co_3O_4 and MnO_2 makes it difficult to separate the individual contributions. The main peak at 300-350 °C probably represents the sum of the processes. The TPR profile of the MMO sample suggests that the redox behaviour of the sample is dominated by the presence of CuO and Co_3O_4, with a secondary contribution of MnO_2.

Regarding the reforming tests, Table 2 shows the yield of four materials in terms of CO and H_2 and CH_4 conversion in the first 2 minutes and 5 minutes of tests. From Table 2 it is evident that the behavior of various samples is different for similar test conditions. After three repeated tests, alternating CH_4 and air regeneration, the best material was Ce-Al both in the first 2 minutes and in the 5 minutes of test at a temperature of 1173 K. The same material also showed the higher H_2 yield at the temperature of 1123 K at the same times. Regarding CH_4 conversion, MMO reported the best value at temperature of 1173 K.

In Table 2 the percentage of carbon according to Eq(3) deposited during the reforming reaction is also shown. For sample Ce-Al and Ce-Cu-Al carbon deposition was negligible. However, for the other samples some C deposition took place. In particular, MMO had the highest values of CH_4 conversion and concurrent carbon deposition. During the regeneration step, carbon was always readily removed by oxidation, as demonstrated by the good repetition of results in subsequent steps.

The images (digital microscope HIROX RH-2000) of the fresh and aged catalysts are compared in Figure 3. The common feature is the formation of macroporosity and cracks, well visible on the catalyst surfaces. The X-ray diffraction analyses of the as-synthesized fresh samples showed that sample Ce-Al, Ce-Cu-Al and Ce-Cu-Ca-Al are composed of the only metal oxides used as starting ingredients. It means that any significant reaction took place during hot consolidation. However, a temperature of 1473 K was set for sample MMO to obtain a single phase cubic final product. Upon testing, the X-ray diffraction patterns of the aged samples present new peaks (i.e., new phases), as consequence of partial oxidation and reforming.

Table 2: ηCO, ηH2 and CH_4 conversion corresponding at first 2 minutes and 5 minutes of reforming

Test #	Bed material	T [K]	Q_{CH4+N2} [L/h]	ηCO	ηH_2	CH_4 conversion	ηCO	ηH_2	CH_4 conversion	Carbon deposition [%]
				2 min			5 min			
1	Ce-Al	1173	76.0	0.60	0.14	0.43	0.85	0.54	0.56	< 0.01
2	Ce-Cu-Al	1173	76.0	0.06	0.03	0.82	0.40	0.32	0.55	< 0.01
3	Ce-Cu-Ca-Al	1173	100.0	0.02	0.03	0.62	0.28	0.36	0.26	1.0
4	Ce-Al	1123	76.0	0.35	0.30	0.26	0.67	0.62	0.16	5.2
5	MMO	1123	92.3	0.01	0.02	0.48	0.35	0.50	0.51	16.5
6	MMO	1173	76.0	0.15	0.08	0.95	0.16	0.10	0.94	26.8

The sample Ce-Cu-Al (Figure 3b) shows the trends of CH_4 and H_2 constant after few minutes without formation of CO_2. Ce-Cu-Ca-Al (Figure 3c) gave rise to decreasing conversion of CH_4 during the 5 minutes of reforming test. Overall, MMO (Figure 3d) exhibited comparatively better performance in terms of CH_4 conversion though a full oxidation reaction seemed to prevail over the partial oxidation producing CO_2 and H_2O instead of CO and H_2. This behavior can be again ascribed to the prompt oxygen provided by the catalyst at the beginning of the reforming stage. The large oxygen release can be reduced by adopting a tuned regeneration, without full replenishment of all O-sites, for instance by lowering the regeneration time, setting lower O_2 partial pressure or using CO_2 as oxidizer (Storione et al., 2024).
The differences in the profiles of the total H_2 and CO produced and the H_2 and CO that should come from partial suggest the formation (and deposition) of solid carbon (Table 2) via CH_4 thermal decomposition in late stage of the reforming step.
Figure 4 shows the transient profiles of volumetric fractions of O_2, CO, CO_2, CH_4 and H_2 sampled at the exit of the reactor during reforming executed at 1173 K. After each reforming stage, the samples were regenerated in air to replenish the initial oxygen content in the catalyst. The profiles, though qualitative, denote some interesting trends. In all cases, at the start of the partial oxidation step, a strong signal of CO_2 was detected. This is caused by the oxygen readily available leading to full oxidization of CH_4 to CO_2 and H_2O (not measured) instead of partial oxidation. Sample Ce-Al (Figure 3a) gave rise to increasing conversion of CH_4, requiring a certain time for being active, thus obtaining an increasing concentration of H_2 and CO and a low concentration of CO_2 (Figure 1a).

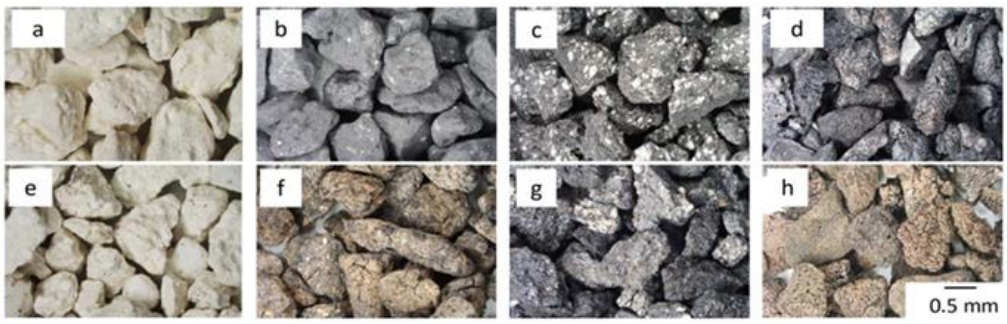

Figure 3: Micrographs by optical microscope of samples: Ce-Al (a,e), Ce-Cu-Al (b,f), Ce-Cu-Ca-Al (c,g), MMO (d,h). Upper and lower rows of micrographs represent, respectively, fresh and aged samples.

4. Conclusions

Four different ceramic catalysts, free from noble elements and toxic compounds, were tested at 1123 and 1173 K for CH_4 conversion to syngas, and showed different behavior in terms of CO, CO_2, H_2 yield and

conversion of CH_4. A value of 94% for the CH_4 conversion at 1173 K was achieved by using the MMO catalyst, based on five oxides and having typical properties of high-entropy solids, that also exhibited high reducibility by TPR analysis. Regarding the yield of CO, the best material was Ce-Al: 85 % and H_2: 62 %, respectively at 1173 K. MMO suffered carbon deposition, whilst Ce-Al and Ce-Cu-Al samples showed negligible coke formation. The oxygen ratio in the feed of the two-steps process governed the trade-off between partial and full oxidation of methane, opening perspectives to process optimization to use CO_2 for the regeneration step. The use of cheap and no-toxic oxides represents a possible incentive to real application.

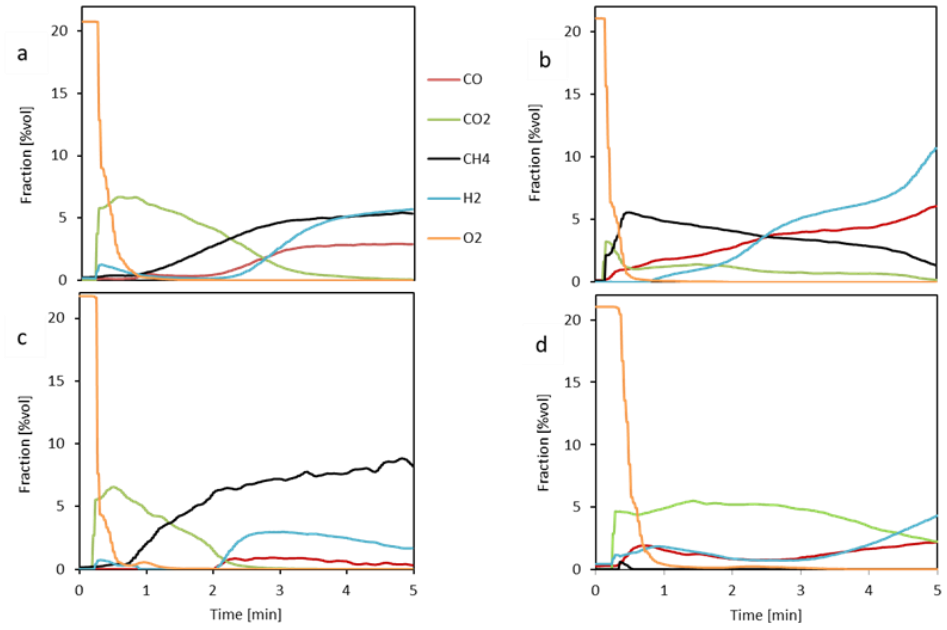

Figure 4: Transient profiles of volumetric fractions of O_2, CO, CO_2, CH_4 and H_2 during reforming at 1173 K*: a) Ce-Al, b) Ce-Cu-Al, c) Ce-Cu-Ca-Al, and d) MMO*

Acknowledgments

The research was funded by the national project on H_2 (AdP Italian Ministery MiTE - ENEA, Mission 2, Comp. 2.3.5, PNRR, 2022-2025, LA 1.1.25).

References

Haotian Zhang, Zhuxing Sun, Yun Hang Hu, 2021, Steam reforming of methane: Current states of catalyst design and process upgrading, Renewable and Sustainable Energy Reviews, 149, 111330.

Guo Z., Wang A., Wang W., Zhao Y.-L., Chiang P.-C., 2021, Implementing Green Chemistry Principles for Circular Economy Towards Sustainable Development Goals, Chem. Eng. Trans., 88, 955-960.

Lunsford J.H., Catalytic Conversion of Methane to More Useful Chemicals and Fuels: A Challenge for the 21st Century, Catal Today 2000, 63, 165–174.

Lyngfelt A., 2013, 20 – Chemical looping combustion (CLC). In: Scala, F. (Ed.), Fluidized Bed Technologies for Near-Zero Emission Combustion and Gasification, Woodhead Publishing, pp. 895–930.

Miccio F., Landi E., Natali Murri A., Minelli M., Doghieri F., Storione A., 2023, Fluidized Bed Reforming of Methane by Chemical Looping with Cerium Oxide Oxygen Carriers, Chem. Eng. Res. Design, 191, 568-577.

Monteverde F., Gaboardi M., 2024, Entropy-driven expansion of the thermodynamic stability of compositionally complex spinel oxides, J. Eur. Ceram. Soc., 44(13), 7704-7715.

Storione A., Boscherini M., Miccio F., Landi E., Minelli M., Doghieri F., 2024, Improvement of Process Conditions for H2 Production by Chemical Looping Reforming, Energies, 17, 1544.

Palma V., Ricca A., Martino M., Meloni E., Intensification Innovative Catalytic Systems for Methane Steam Reforming, Chem. Eng. Trans., 52, 301-306,2016.